Jewel Journal of Scientific Research (JJSR) 5(1&2): 128–141, 2020
©Federal University of Kashere-Nigeria (Print ISSN: 2384 – 6267, Online ISSN 2756-651X)
jjsr.fukashere.edu.ng

Appraisal of Aquifer Protective Capacity and Soil Corrosivity Using Electrical Resistivity Method in Miango Area, Jos, Plateau State, Nigeria

Bulus, J. A. [1]*,Odewumi, S. C. [2], Kaze, I. N. [1] and Abalaka, I. E. [1]
[1]Department of Geology, Faculty of Natural Sciences, University of Jos, Jos, Nigeria.
[2]Department of Science Laboratory Technology, Faculty of Natural Sciences, University of Jos
*Corresponding author E-mail: bulusjosephazi@gmail.com

Abstract
A geophysical survey was carried out in Miango area, Bassa Local Government Area of Plateau State, northcentral Nigeria using Electrical resistivity soundings. This study aimed at delineating zones that are very prone to groundwater contamination from surface contaminants and subsurface soils that are corrosive to utility pipes. Schlumberger configurations were employed to delineate the subsurface geologic layers, corrosivity level and aquifer protective capacity. Five (5) transverses were mapped out along which thirty-nine (39) Vertical Electrical Sounding (VES) data were acquired using D.C. SAS 2000 resistivity meter with half-current electrode separation (AB/2) of 1 to 125 m. The interpretations of the data collected were aided by computer assisted iterative using 1-D inversion technique (IX1D), MS Excel 2016 and surfer 11 software. Sounding curve types observed in the area are mostly the QH, H, and HA curves. Five (5) distinct geoelectric layers were identified namely: topsoil, clayey layer, laterite, fractured basement and fresh basement. The measured overburden thickness ranges from 0.78 to 42 m and the longitudinal conductance of the overburden units ranging from 0.002142 to 1.260121 mhos. The pink colour region have relatively high topsoil resistivity value and is practically noncorrosive, while the green colour region is slightly corrosive. Based on the longitudinal conductance values; poor, weak, moderate and good aquifer protective capacity zones were defined. The poor and weak protective capacity zones are vulnerable to surface contamination while the moderate and good protective capacity zones have higher protective property to prevent contaminated fluids infiltrations into the aquifer.

Key Words: Aquifer Protective Capacity, Dar-Zarrouk parameters, Overburden thickness, Schlumberger array and Soil corrosivity.

Received: 16th Aug., 2020 *Accepted:* 5th Dec, 2020 *Published Online:* 25th Dec, 2020

Introduction

Geophysical methods are applied in a wide range of applications which include roads, dams and dikes constructions. Since the last decade, the involvement of geophysics in civil and environment engineering has become auspicious approach (Luma and Jadi, 2000; Othman, 2005). At present, standard engineering practices require investigation of the subsurface at engineering construction sites. In baseline studies for pipe-laying programmes, issues relating to the corrosivity of the host soil and possible effects on underground pipes in an environment are examined (Agunloye, 1984).

Soil corrosion is a complex phenomenon with multitude variables. Several chemical actions and reactions occur between the laid pipes and the host soil. Unfortunately, site engineers sometimes fail to incorporate predevelopment geophysical

investigations in their job plan for reasons of cost and other logistic considerations despite their necessity (Olorunfemi *et al.*, 2000).

One of the simplest measurable and pragmatic classifications is founded on soil resistivity. Knowledge of the resistivity of the surrounding soil gives an indication of the corrosiveness of the soil layer. Sandy soil is high up on the resistivity scale due to their inadequate water storage capacity and high porosity. Hence, it is considered the least corrosive. On the other hand, Clay soils especially those contaminated with salty water are on the opposite end of the resistivity range (Olorunfemi *et al.*, 2004).

The study area is underlain by Precambrian Basement rock sand these rocks are inherently characterized by low porosity and near negligible permeability. Miango is a fast-growing settlement with increase in population and the progressive infrastructural development within the community daily emphasize the need for the development of a sustainable water supply network. The aim of the study is to investigate and estimate the corrosivity of the subsurface materials in Miango area with a view to delineate the subsurface geologic layers and as well determine their corrosion severity using the electrical resistivity method

Location and Geology of the Study Area

The study area is located within Latitudes 840700 to 841710 N and Longitudes 753800 to 755080 E in Universal Traverse Mercator (UTM) and occurs in Miango area of Bassa Local Government Area of Plateau State. The area is generally accessible through the Jos-Miango road with some minor roads and foot paths linking the various communities (Fig. 1). The topography is relatively undulating with elevation ranging from 356 to 375 m above sea level and part of the study area is drained by streams and river. The Geology of the study area was explained within the context of the Geology of the Precambrian Basement Complex of northcentral Nigeria which form a part of the Basement Complex of Nigeria (Rahaman, 1976). The major rock units within the area are Newer Basalt, Miango biotite granite, porphyritic biotite and biotite hornblende granite (Fig. 2).

Materials and Methods

The geophysical data were acquired with the D.C. SAS 2000 resistivity meter that contains both the transmitter unit, through which current enters the ground and the receiver unit, through which the resultant potential difference was recorded. Other materials used for geophysical survey include: two each of metallic current electrodes and potential electrodes; two red coloured connecting cables for current and two black coloured cables for potential electrodes; two reels of calibrated rope; hammer for driving the electrodes into the ground; compass for finding the orientation of the traverses; cutlass for cutting traverses and data sheet for recording the field data.

Schlumberger configuration was employed in the data gathering process known as Vertical Electrical Sounding (VES) as described by Ariyo and Adeyemi (2009); Ajibade and Ogungbesan (2013); and Emmanuel *et al.,*(2015).Schlumberger VES investigation measures the changes in formation resistivity with depth and electrode spread of AB/2 was varied from 1 to 125 m. It requires that current electrodes spacing, AB is increased after every reading while potential electrodes spacing, MN is kept constant for most readings but increased when necessary using the control AB/2 > MN/2 (Okolie *et al*., 2010). The Schlumberger array was sounded using the terrameter from which apparent resistivity data of the subsurface under investigation were gotten with changing current electrode separations along each traverse at designated stations.

Thirty-nine (39) VES readings were acquired from the study area and were interpreted with the aid of computer assisted iterative using 1-D inversion technique software (IX1D, Interpex, USA). The software was further used for both computer iteration and modeling. Computer iteration was carried out to decrease errors to an anticipated limit and to improve the goodness of fitting between the field data and the computer-generated model.

The Dar-Zarrouk parameters were obtained from the first order geoelectric

parameters (i.e. layer resistivities and thicknesses). The Total longitudinal unit conductance (S) is particularly important when is used to describe a geoelectric section consisting of several layers. The total longitudinal conductance (S) of the overburden unit at every vertical electrical sounding location was obtained from the mathematical equation according to Zhody *et al.,* (1974) as shown in equation 1. For n layers, the total longitudinal unit conductance is:

$$S = \sum_{i=1}^{n} \left(\frac{hi}{\rho i}\right) = h1 / \rho 1 + h\,2 / \rho\,2 + \ldots + h\,n / \rho\,n \quad \ldots\ldots\ldots\ldots\ldots\ldots (1)$$

Where hi is the layer thickness, *pi* is layer resistivity whiles the number of layers from the surface to the top of aquifer, (*i*) vary from 1 to n.

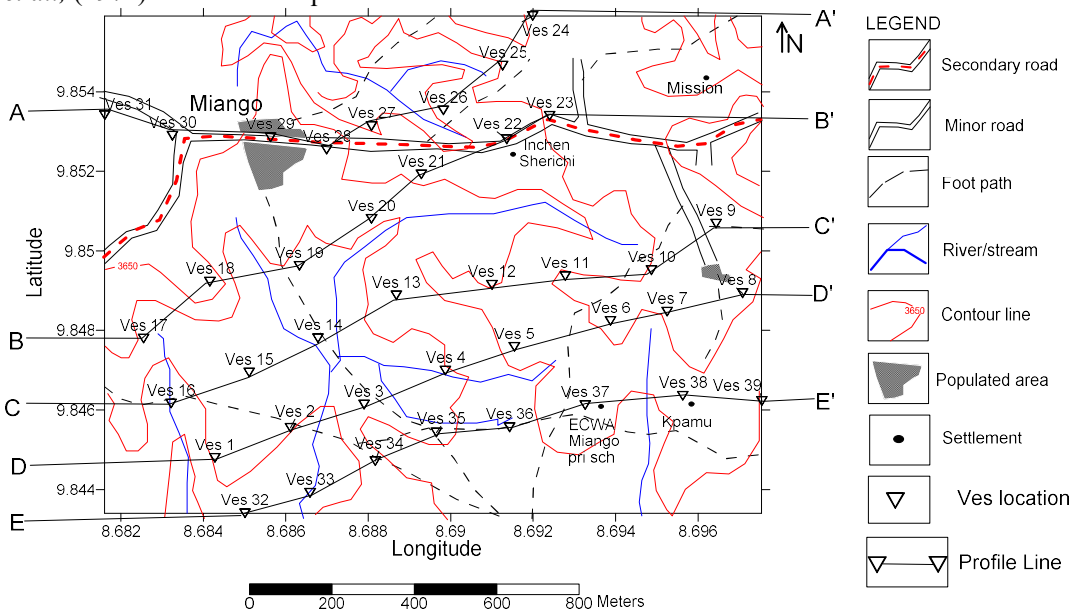

Figure 1: Topographical Map of Miango and environs with location of VES points and profile lines

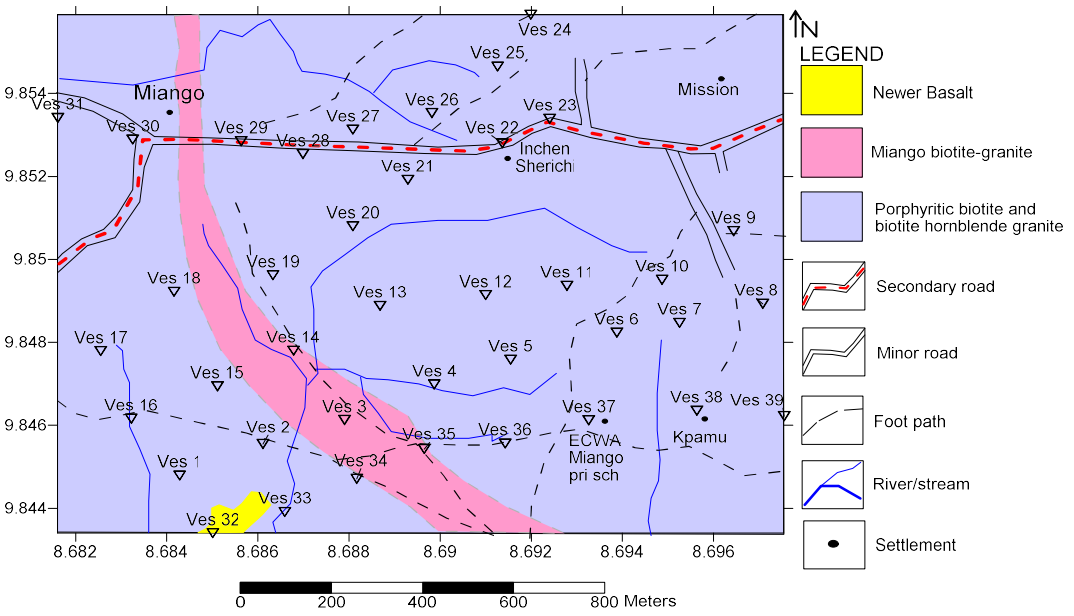

Figure 2: Geological Map of Miango and environs with location of VES points

Results and Discussion

The true resistivity for each layer (ρ), true thickness for each Layer (h), typical curve types, Total Longitudinal Conductance Unit(S) and aquifer thickness are presented in Table 1. The summary of the VES interpretations for the thirty-nine (39) VES stations are presented in Table 1.Figures 3a to 3c were obtained from the interpretation of the data with the aid of computer assisted iterative using 1-D inversion technique software (IX1D, Interpex, USA).

Aquifer Protective Capacity Evaluation

The nature of the materials that overlain the mapped aquifers were evaluated using primary electrical parameters such as resistivity and thickness. The longitudinal unit conductance (S) was used to determine its capacity to prevent infiltration of unwanted fluids into the aquifer. The longitudinal unit conductance map was derived from equation (1) for the thirty-nine (39) VES locations (Fig. 4).

The longitudinal unit conductance (S) value of the study area ranges from 0.002142 to 1.260121 mhos and were used for the overburden protective capacity rating. According to the classification of Henriet, (1976) and Oladapo *et al*., (2004); the study area was classified into four (4) protective capacity zones namely: good, moderate weak and poor protective capacity as shown in Figure 4. Where the conductance is greater than 0.7 mhos are considered zones of good protective capacity. The portion having conductance values ranging from 0.2 to 0.69 mhos was classified as zone of moderate protective capacity; and area with values ranging from 0.1 to 0.19 mhos were classified as exhibiting weak protective capacity while the zones where the conductance value is less than 0.1 mhos were considered to have poor protective capacity (Fig. 4).

The present research indicates that the overburden materials in the area around the pink and cyan colours portions of the study area have good to moderate protective capacity (Fig. 4) and relatively thick overburden between 26 to 42 m thick (Fig. 5) while the green and yellow colour areas show weak to poor overburden protective capacity (Fig. 4) and thin overburden thickness. Figure 4 further shows that about 64.10% of the study area falls within the poor to weak overburden protective capacity, while about 35.90% of the area constitute the moderate to good protective capacity.

The areas covered by poor and weak Aquifer protective capacity regions of the study area will be vulnerable to surface contamination sources such as infiltration of leachates from decomposition of open refuse dumps, leakage from underground petroleum storage tanks and diffuse pollution from agricultural activities. The good (pink colour) and moderate (cyan colour) aquifer protective capacity zones of the study area have higher protective property to prevent contaminated fluids infiltrations into the aquifer so that in the face of contamination such zones are seemingly safe.

The earth materials act as a natural filter to infiltrated liquid; therefore, its capability to preclude and filter percolating ground surface polluting fluids is a measure of its protective capacity (Adeniji *et al.,* 2014; Olorunfemi *et al.,* 1999). The geologic materials overlying an aquifer could act as protection in preventing the fluid from infiltrating into it. The highly impervious clayey overburden characterized by relatively high longitudinal conductance similar to good protective zone (Fig. 4) offers protection to the underlying aquifer (Abiola *et al.,* 2009).

Table1. Calculated geoelectric (Dar-Zarrouk) parameters

	Resistivity (Ohm-m)					Thickness (m)						
VES station	ρ_1	ρ_2	ρ_3	ρ_4	ρ_5	h_1	h_2	h_3	h_4	**Curve type**	**Longitudinal Conductance (mhos)**	**Aquifer thickness**
1	632.09	6.33	797.26	49.47		0.7	0.7	22		HK	0.111692	40.96
2	584.74	97.52	128.03			2.8	24.9			H	1.260121	38.82
3	2032	180.54	641.38	44447		0.4	10.4	8.4		HA	0.057802	8.00
4	2145.8	791.8	9001.1	8.41		1.4	9.6	7.2		HK	0.013577	23.47
5	275.30	72.25	220.72			0.8	5.3			H	0.762623	40.87
6	1666.80	407.38	91.01	1447.40	18.61	0.8	9.5	5.9	17.5	QHK	0.088628	7.97
7	422.88	73.54	163.53	78122		1.4	1.1	14.4		HA	0.218268	24.77
8	1817.7	581.14	321.12			2.5	30			Q	0.052998	39.17
9	282.69	133.80	38.11	466.78		1.1	8	5.2		QH	0.063682	40.57
10	1187.20	128.16	267.76	29469		0.9	4.5	25.8		HA	0.132225	30.3
11	245.32	56.25	1905.60			3.3	11.5			H	0.917896	30.37
12	1444.90	431.46	80.33	290.91		0.9	5.1	4.2		QH	0.012443	40.77
13	312.17	57.54	84.40	175.54		0.5	1.1	15.2		HA	0.200814	41.17
14	4774.20	932.82	337.49	39.98		0.5	1.9	18.4		QQ	0.002142	41.17
15	545.84	165.35	29.39	370.38	8.12	0.9	6.4	6.9	18	QHK	0.275128	40.77
16	1912.80	596.73	115.55	1622.60	15.63	1.0	3.2	14.5	17.2	QH	0.131372	17.7
17	109.96	26.30	33.39	985.78	28.59	0.6	4.3	10.6	17.2	HAK	0.686415	41.07
18	1136.30	18.41	63.34	167.83		0.4	0.5	16.5		HA	0.027511	41.27
19	807.90	289.48	24.27	219.08		0.7	5.9	4.8		QH	0.219023	40.97
20	137.88	40.98	144.52	99.76		0.7	5.3	9.9		HK	0.762623	40.97
21	1625.0	40.66	175.73			2.2	3.1			H	0.575959	39.47
22	596.21	360.82	16.94	8410.2		0.9	7.2	6.2		QH	0.021464	13.4
23	976.93	126.85	26.43	547.08		1.6	4.8	4.6		QH	0.213522	40.07
24	226.95	124.03	14624	53.40		1.2	18	4.7		HK	0.150414	18.00
25	301.55	5245	811.17	425.65		0.2	0.3	14.0		KQ	0.017979	41.17
26	906.04	88.55	318.86			1.9	15.3			H	1.074881	39.77
27	342.15	144.96	325.70			1	27			H	0.189181	40.67
28	399.76	284.09	62.84	826.89	92.57	0.8	2.4	10.8	25	QHK	0.182314	40.70
29	124.67	34.69	810.06	4.72	115.14	1.2	2	2.7	2.1	HKH	0.030612	40.47
30	144.70	586.70	344.58	34114		4.5	6.5	27.5		KH	0.042178	34.00
31	173.29	24026	379.29			3.3	0.1			K	0.019047	38.27
32	1314.40	291.52	599.19	52645		2.2	4.6	25.4		HA	0.017453	30.00
33	2384.30	262.14	74.19			0.5	3.2			Q	0.012417	41.17
34	497.56	0.32	5042.10			4.2	8			H	0.844119	8.00
35	961.29	427.77	1605.7	305.02		1.4	8.8	13.4		HK	0.022028	18.07
36	1656.5	376.98	22.57	22493		1.7	8.3	6.6		QH	0.315467	14.90
37	1345.80	672.54	113.30	339.74		1.8	10.2	5.8		QH	0.016504	39.87
38	328.43	654.64	67.59	3481.60		1.1	4.7	5.2		KH	0.087463	9.90
39	105.64	1774.30	349.64	448.75		0.5	0.3	19.4		KH	0.004902	40.87

VES = vertical electrical sounding, ρ_1= first layer resistivity, ρ_2= second layer resistivity, ρ_3= third layer resistivity ρ_4= fourth layer resistivity, ρ_5= fifth layer resistivity, h_1= first layer thickness, h_2= second layer thickness, h_3= third layer thickness, h_4= fourth layer thickness, m = meters.

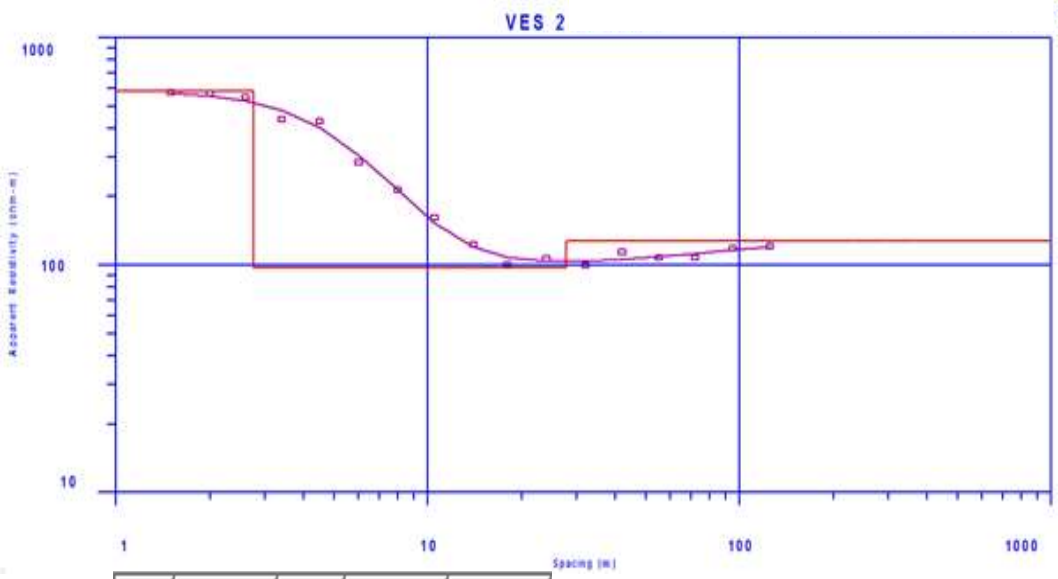

#	Rho	Fix?	Thick	Depth
1	584.74	☐	2.7659	2.7659
2	97.518	☐	24.977	27.742
3	128.03	☐		
4		☐		

Figure 3a: Typical H curve type for VES 2

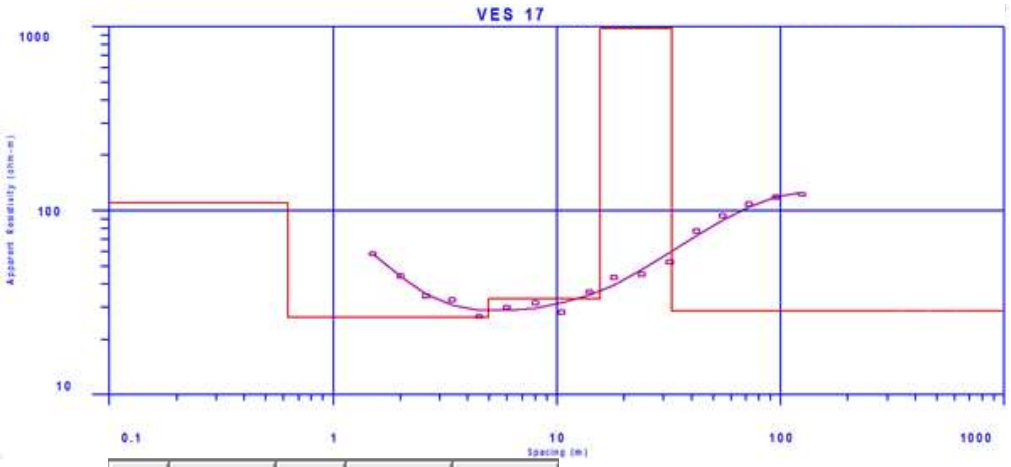

#	Rho	Fix?	Thick	Depth
1	109.96	☐	0.62632	0.62632
2	26.302	☐	4.3145	4.9408
3	33.397	☐	10.628	15.569
4	985.78	☐	17.212	32.781
5	28.599	☐		
6		☐		

Figure 3b: Typical HAK curve type for VES 17

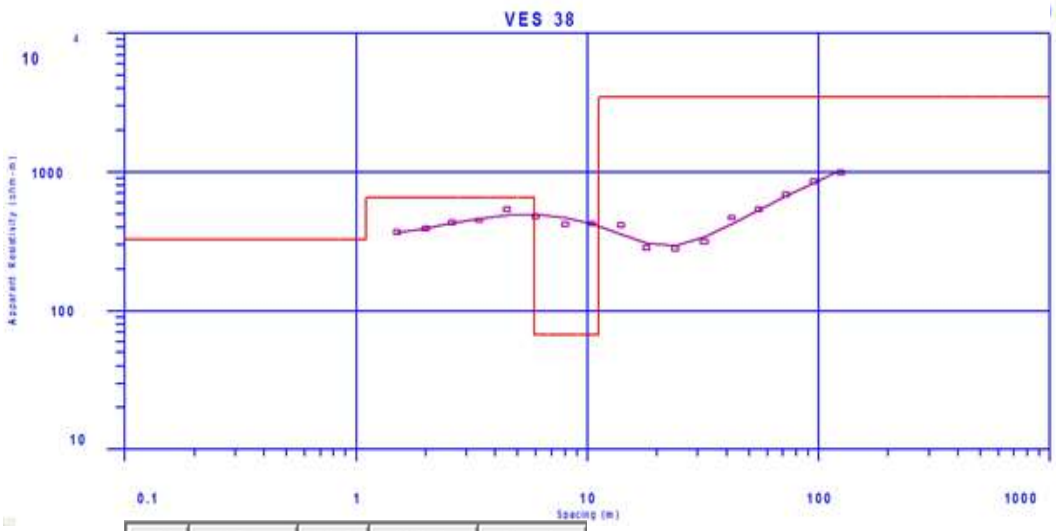

#	Rho	Fix?	Thick	Depth
1	328.43		1.1074	1.1074
2	654.64		4.7822	5.8895
3	67.590		5.2839	11.173
4	3481.6			
5				

Figure 3c: Typical KH curve type for VES 38

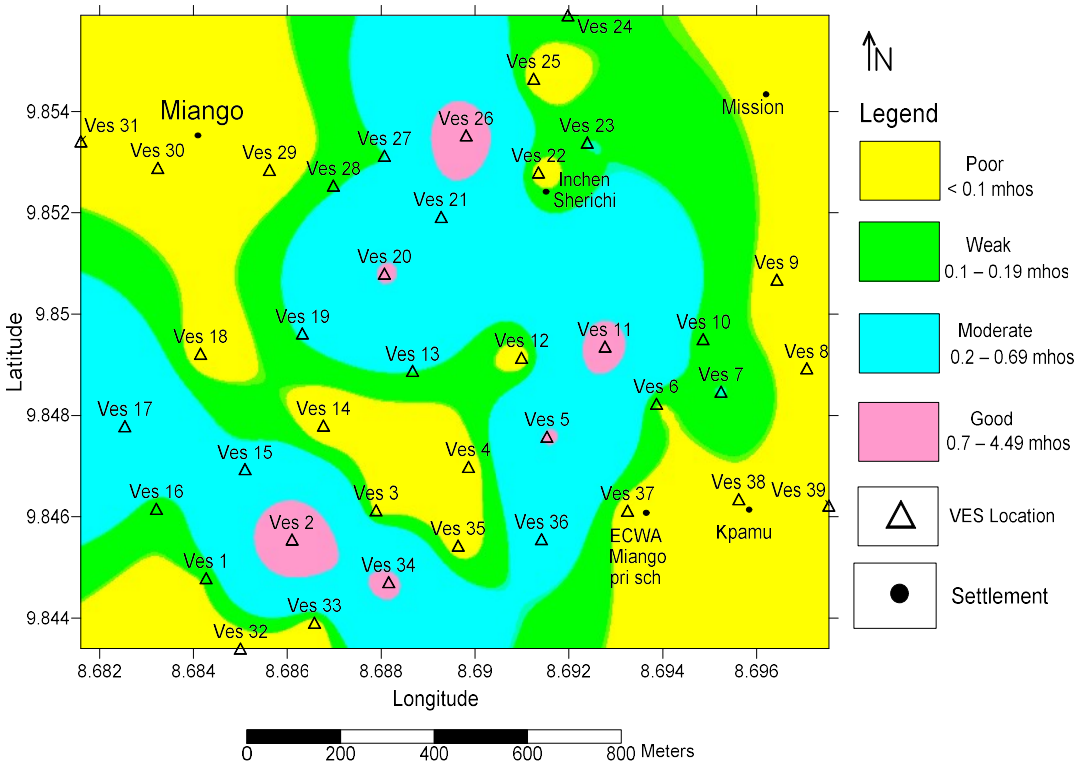

Figure 4: Aquifer protective capacity map of the study area.

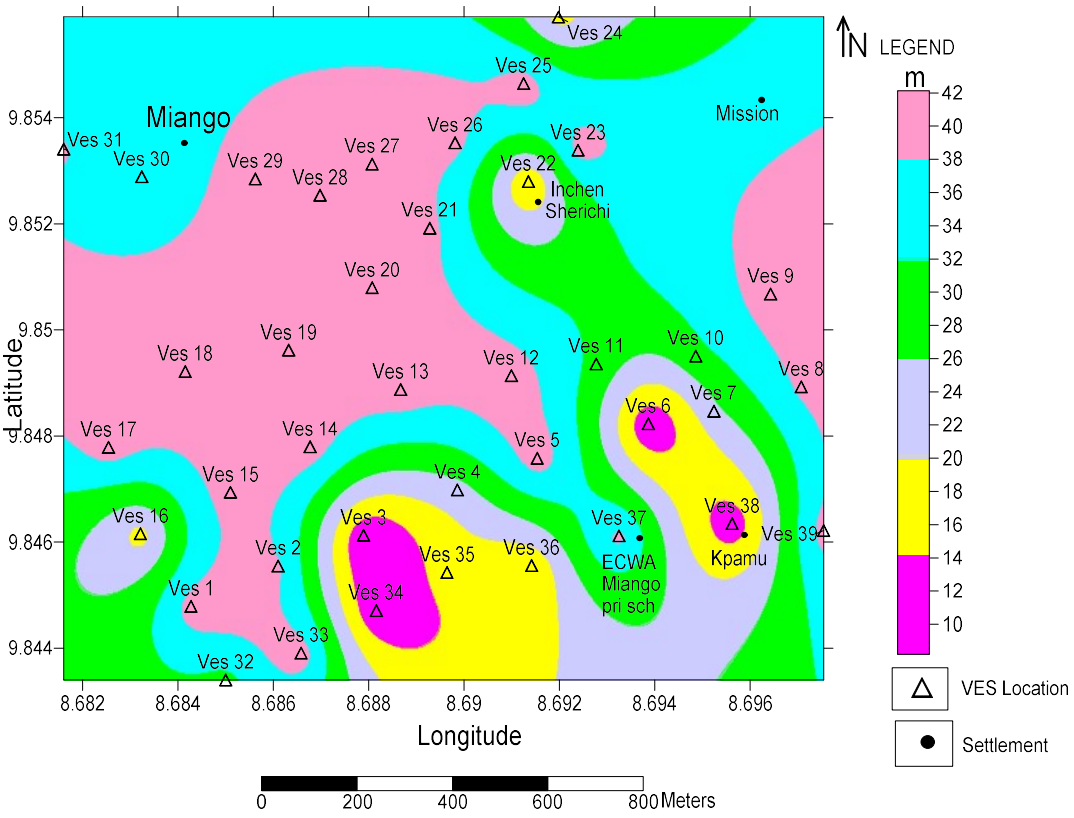

Figure 5: Overburden thickness map of the study area.

Evaluation of Soil Corrosivity

The interpretations of the VES results obtained from the topsoil (first layer) resistivity values were used in estimating the corrosivity of the subsoils in the study area. The classification of soil resistivity in terms of corrosivity in Miango area as shown in Figure 6 was done according to the classification of Baeckmann and Schenwenk (1975); Agunloye (1984); and Oladapo *et al.* (2004). The thickness of the top layer ranges from 0.2 m (VES 25) to 4.5 m (VES 30) whereas the resistivity (Table 1) ranges from 105.64 Ωm (VES 39) to 2384.30 Ωm (VES 30).

Resistivity values of >180 Ωm indicating practically noncorrosive was observed around the area with pink colour while resistivity values of 60 to 180 Ωm indicating slightly corrosive was observed in the area with green colour as shown in Figure 6. The resistivity values obtained from the area (105.64 -2384.30 Ωm) exceeded the resistivity values of 10 to 60 Ωm (yellow colour) for areas indicating moderately corrosive and <10 Ωm (cyan colour) for areas indicating very strongly corrosive (Fig. 6). This indicates that moderately corrosive and very strongly corrosive zones were not identified in Miango area

Civil engineering construction works mostly comprises lying of metallic pipes. Buried pipes are vulnerable to corrosion and subsequent failure if the host soil medium is aggressive and corrosive (Akintorinwa and Abiola, 2011).Most civil utility pipes and engineering foundations are buried within the topsoil layer region.

Topsoil resistivity values of Miango area ranges from 105.64 to 2384.30 Ωm and this further indicates that the topsoil corrosivity varied from 'practically noncorrosive' to 'slightly corrosive'. Over 84.62% of the study area (pink colour) has relatively high topsoil resistivity values with low tendency for corrosivity. Only about 15.38% in the study area (green colour) is 'slightly' corrosive. The topsoil observed within the slightly' corrosive (green colour) area will make metallic pipes/utility buried in them to be slightly susceptible to corrosion.

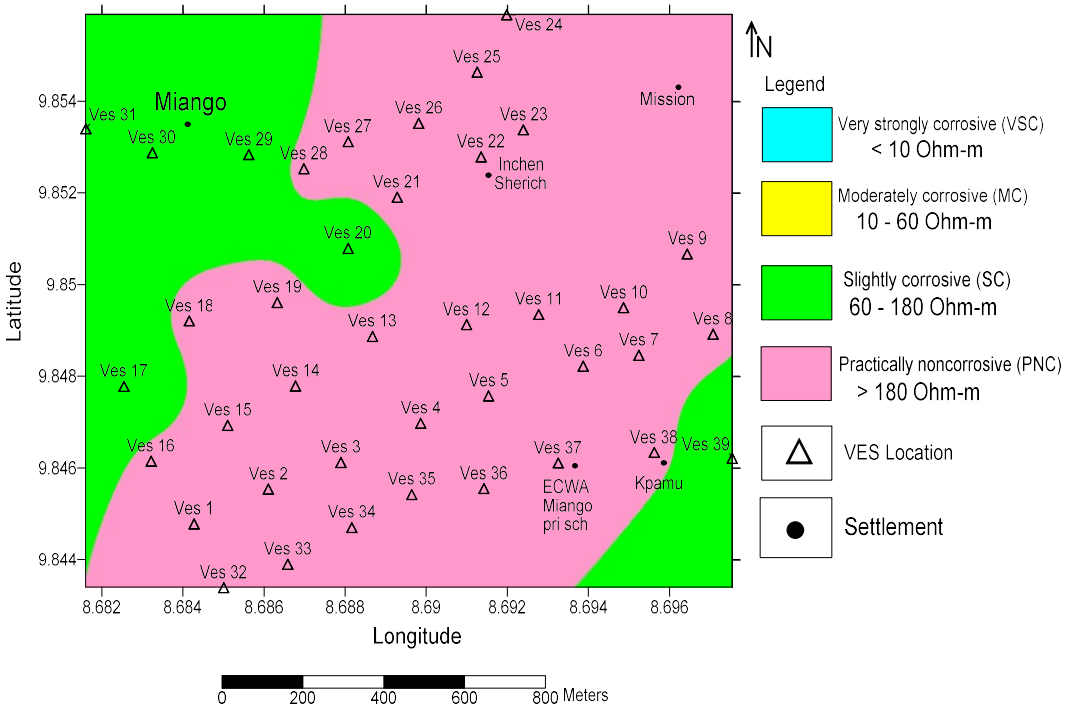

Figure 6: Soil corrosivity map of the study area.

Geoelectric Sections

The summary of the results of the thirty-nine (39) Vertical Electrical Soundings (VES) carried out in the study area is presented in Table 1. Figure 7a shows the Profile 'A-A' section and has five (5) distinct geologic layers. The topsoil has resistivities values of 173.29 to 906.04 Ω-m and thickness ranging from 0.2 to 4.5 m. The second layer consists of laterite at VES 31 and VES 25, with clayey layer at VES 26 and VES 29 that directly underlying the topsoil having resistivities of 124.03 to 24026 Ω-m and thickness of 0.1to 18 m.

The third layer consists of fractured basement having resistivities of 62.84 to14624 Ω-m and thickness of 2.7 to 10.5 m. The fourth layer is made up of fractured/fresh basement having resistivities 53.40 to 24026 Ω-m and thickness of 0.1 to 18 m. The fifth layer of an infinite depth has resistivities values in the ranges of 92.57 to 115.14 Ω-m **(**Fig. 7a). Aquifer at VES 26 and VES 29 are protected from surface fluid contaminants due to thick clay layer overlying the aquifer and the entire profile is good for borehole drilling as a result of very thick aquifer and deeper basement rock (Fig. 7a).

The Profile B-B' section is shown in Figure 7b and has four (4) distinct geologic layers. The topsoil resistivities range from 109.96 to 1136.30 Ω-m with thickness of about 0.4 to 2.2 m. The second layer has clayey unit at VES 17, VES 18, VES 20 and VES 21 underlying the topsoil with resistivities of 18.41 to 360.82 Ω-m and thickness of 0.5 to 7.2m. The fracture basement with resistivities value ranges from16.94 to 175.73 Ω-m and thickness ranging from 4.6 to 16.5 m was identified at the third layer. The fourth layer has fresh basement at VES 22 with resistivities value of 8410.20 Ω-m and an infinite thickness. The clay layer underlying the topsoil was located at VES 17, VES 18, VES 20 and VES 21 which serves as a seal for the aquifer **(**Fig. 7b). VES 22 has thin overburden thickness and will not be favourable for groundwater production while VES 19, VES 22 and VES 23 are vulnerable to fluid contamination as they are devoid of protective sealed above their aquifer.

Figure 7c shows Profile 'C-C' section and has four (4) distinct geologic layers. The topsoil layer has resistivities of 245.32 to 1912.80 Ω-m and thickness ranging 0.5 to3.3 m. The second layer consists of clayey layer underlying the topsoil at VES

11 and VES 13 with resistivities of 56.25 to 932 Ω-m and thickness of 1.1to11.5 m. The third layer consists of fractured/fresh basement at VES 11, with resistivities ranging from 38.11 to 1905.60 Ω-m and thickness ranging from 4.2 to 25.8 m. The fourth layer has fresh basement at VES 10 and VES 16 with resistivities ranging from 1622.60 to 29469 Ω-m and an infinite thickness (Fig. 7c). VES 11 has clay layer overlying the fracture basement and VES 13 has clay layer overlying the fresh basement while VES 10 and VES 16 have fractured basement overlying the fresh basement. VES 11 will not be favourable for borehole drilling due to clay layer aquifer which is not permeable.

The Profile 'D-D' section is shown in Figure 7d and has four (4) distinct geologic layers. The topsoil has resistivities of 275.30 to 2145.80 Ω-m and thickness of 0.4 to 2.8 m. The second layer consists of clayey layer underlying the topsoil at VES 1, VES 2, VES 5 and VES 7 with resistivities of 6.33 to 791.8 Ω-m and thickness of 0.7 to 24.9 m. The third layer consists of fractured/fresh basement having resistivities of 91.01 to 9001.1 Ω-m and thickness of 5.9 to 22 m. The fourth layer has fresh basement at VES 3, VES 6 and VES 7 with resistivities ranging from 1447.40 to 44447 Ω-m and an infinite thickness (Fig. 7d). Productive borehole can be sited at VES 1, VES 4, VES 5 and VES 8 with clay layer overlying the aquifer at VES 1 and VES 5 that will serve as sealed.

Figure 7e shows the Profile E-E' section and has five (5) distinct geologic layers. The topsoil has resistivities value of 105.64 to 1656.5 Ω-m and thickness of 0.5 to 4.2 m. The second layer consists of laterite at VES 39 and clayey layer (third layer) at VES 34 that directly underlying the topsoil having resistivities of 0.32 to 1774.30 Ω-m and thickness of 0.3 to 10.2 m. The fourth layer consists of fractured/fresh basement located at VES 35 having resistivities of 22.57 to 1605.7 Ω-m and thickness of 5.2 to 25.4 m. The fifth layer was located at VES 32, VES 36 and VES 38 having resistivities value ranges from 1447.40 to 44447 Ω-m with an infinite depth (Fig. 7e). The aquifer with thin overburden was located at VES 36 and VES 38 but not recommended for borehole production.

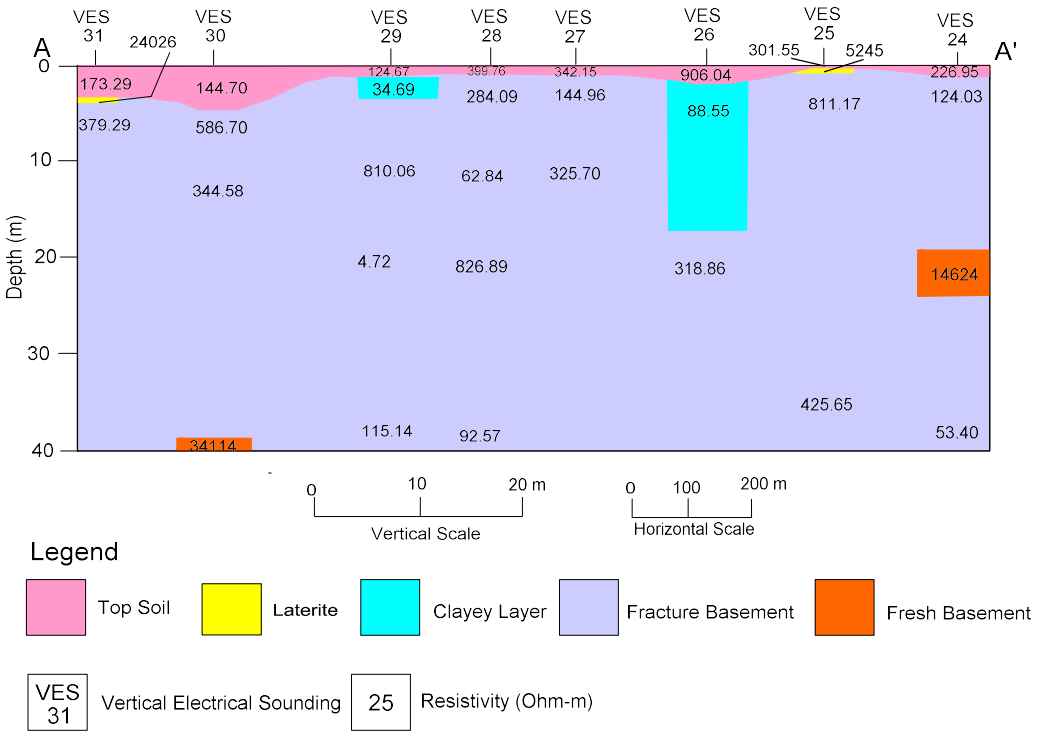

Figure 7a: Geoelectric section for Profile A-A'.

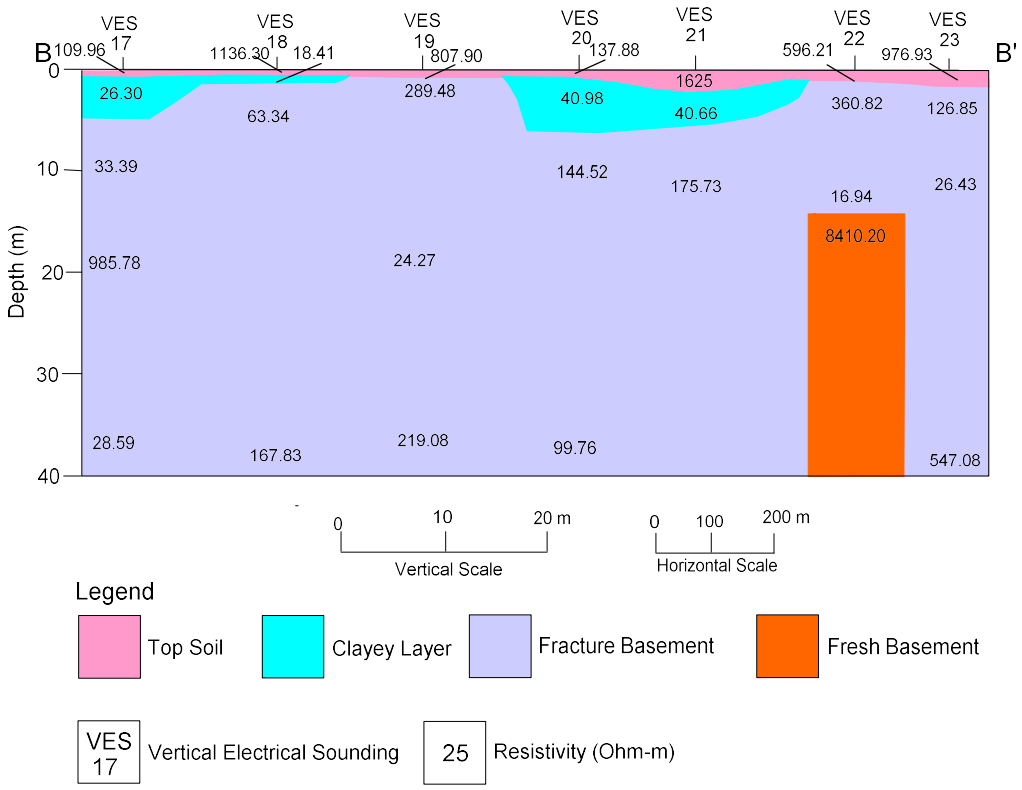

Figure 7b: Geoelectric section for Profile B-B'.

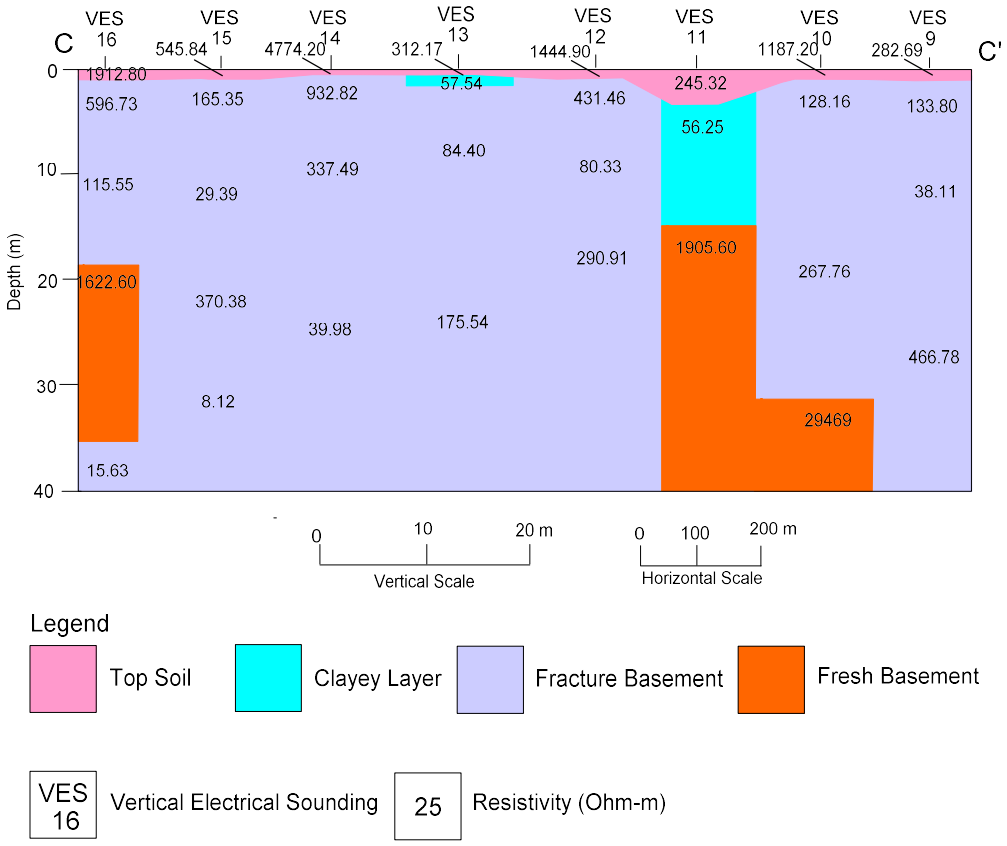

Figure 7c: Geoelectric section for Profile C-C'.

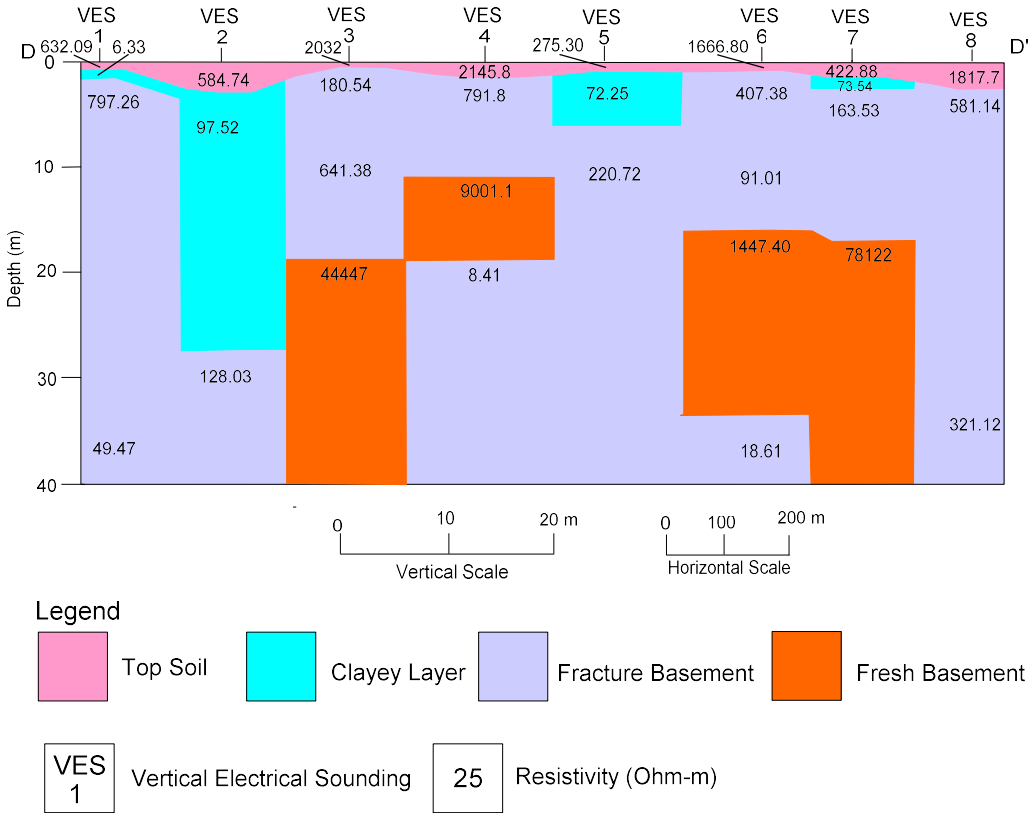

Figure 7d: Geoelectric section for Profile D-D'

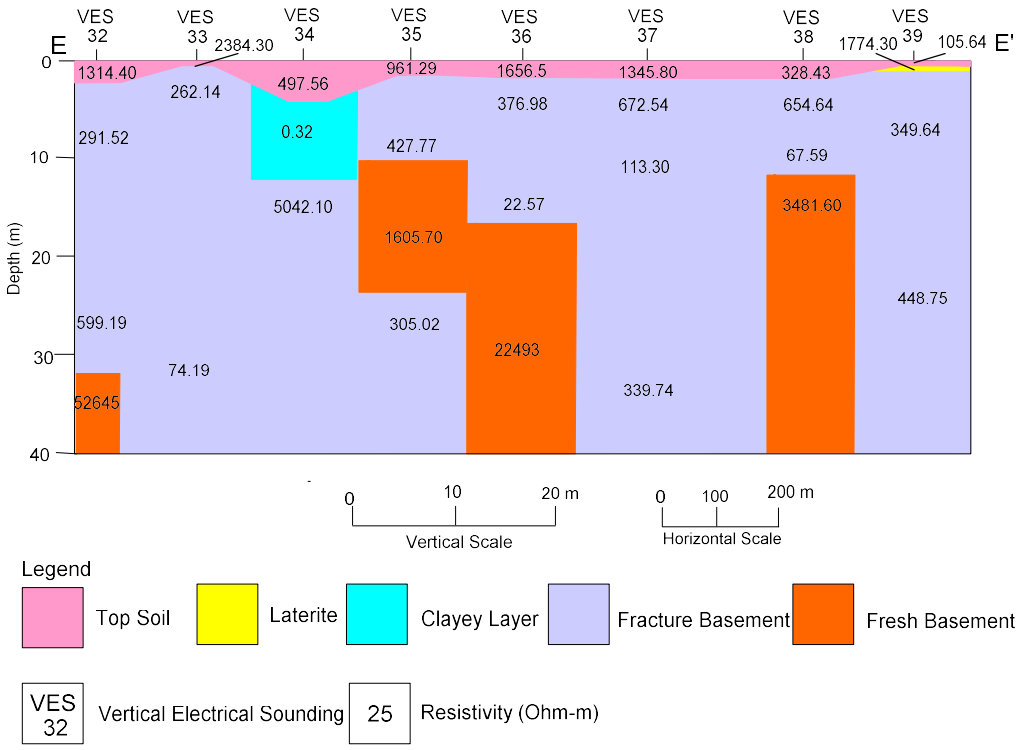

Figure 7e: Geoelectric section for Profile E-E'.

Conclusions

The five (5) distinct subsurface geologic layers have been identified in the area namely: the topsoil, laterite, clayey layer, fractured basement and the fresh basement. The study area was classified based on the values of longitudinal unit conductance into four (4) protective capacity zones namely: good, moderate, weak and poor. The areas covered by poor and weak aquifer protective capacity regions will be vulnerable to surface contamination sources while good and moderate aquifer protective capacity zones have higher protective property to prevent contaminated fluids infiltrations into the aquifer. The Topsoil resistivity values indicate that the topsoil corrosivity varied from practically noncorrosive to slightly corrosive. Thus, the topsoil within the slightly corrosive area will make metallic pipes/utility buried in them to be slightly susceptible to corrosion.

References

Adeniji, A. E., Omonona, O. V., Obiora, D. N. and Chukudebelu, J. U. (2014). Evaluation of soil corrosivity and aquifer protective capacity using geoelectrical investigation in Bwari basement complex area, Abuja," *Journal of Earth System Science,* 123 (3): 491–502.

Ajibade, O. M. and Ogungbesan, G. O.(2013). Prospects and Quality Indices for Groundwater Development in Ibadan Metropolis, Southwestern, Nigeria. *International Journal of Development and Sustainability,* 2 (1): 398 - 414

Ariyo, S. O and Adeyemi, G. O. (2009). Role of Electrical Resistivity Method for Groundwater Exploration in Hard Rock Area; A case study from Fidiwo/Ajebo Area of Southwestern, Nigeria. *The pacific Journal of Science and Technology,* 10 (1): 483–486.

Akintorinwa, O. J and Abiola, O. (2011). Subsoil evaluation for pre-foundation study using geophysical and geotechnical approach; *Journal of Emerging Trends Eng. Applied Science.* 2 (5): 858–863.

Agunloye, O. (1984). Soil aggressivity along steel pipeline route at Ajaokuta southwestern Nigeria. *Journal of Mining Geology*. 21**:** 97–101.

Baeckmann, W.V and Schwenk, W. (1975). Handbook of cathodic protection: The theory and practice of electrochemical corrosion protection technique; Surrey Protucullin Press.

Emmanuel, O. O., Adelowo, A. and Amao, E. (2015). Determination of Groundwater Potential in the Permanent site of University of Abuja, FCT, Nigeria, *International Journal of Innovation and Scientific Research*, 16 (2): 313-325.

Henriet, J. P. (1976). Direct application of the Dar Zarrouk parameters in groundwater surveys; *Geophysical Prospect*. 24: 344 - 353.

Luna, R. and Jadi, H. (2000). Determination of dynamic soil properties using geophysical methods. Proc 1st International Conference on the Application of Geophysical and NDT

Methodologies to Transportation Facilities and Infrastructure Geophysics *Federal Highway Administration*, Saint Louis, M.O., 3: 1 - 15.

Oladapo, M. I., Mohammed, M. Z., Adeoye, O. O. and Adetola, O. O. (2004): Geoelectric Investigation of the Ondo-State Housing Corporation Estate Ijapo Akure, southwestern

Nigeria, *Journal of Mining Geology*, 40 (1): 41–48.

Okolie, E.C., Atakpo, E. and Okpikoro, F. E. (2010). Application of linear Schlumberger configuration in delineation of formation strata and groundwater distribution in Ifon Ondo State Nigeria, *International Journal of Physical Sciences*, 5 (6): 642-650

Olorunfemi, M, O., Ojo, J. S. and Akintunde, O. M. (1999). Hydrogeophysical evaluation of the groundwater potential of Akure metropolis, southwestern Nigeria.

International Research Journal of Geology and Mining, 35 (2): 207-228.

Olorunfemi, M. O., Ojo, J. S., Sonuga, F.A., Ajayi, O. and Oladapo, M. I. (2000). Geoelectric and electromagnetic investigation of the failed koza and Nassarawa earth dams around Kastina, Northern Nigeria. *Journal of Mining and Geology,* 36 (1): 51 - 65.

Olorunfemi, M.O., Idornigie, A.I., Coker, A.T. and Babadiya, G.E. (2004). On the application of the electrical resistivity method on foundation failure investigation –a case study. *Global Journal of Geological Sciences*, 2 (1): 139 – 151.

Othman, A.A.A. (2005). Construed geotechnical characteristics of foundation beds by seismic measurements, *Journal of Geophysical Engineering,* 2: 16 - 138.

Rahaman, M. A. (1976). Review of basement geology of south western Nigeria. In: *Geology of Nigeria* ed. Kogbe C. A. Elizabethan Pub. Lagos, Nigeria, 41–58

Zohdy, A. A. R., Eaton, G. P. and Mabey, D. R. (1974). Application of surface geophysics to groundwater investigations. In *Techniques of Water Resources Investigations of the United States Geological Survey,* Book 2, Chapter D1, 63.